LAMONT-DOHERTY GEOLOGICAL OBSERVATORY

OF COLUMBIA UNIVERSITY

PALISADES, NEW YORK

T E C H N I C A L R E P O R T

For the

EARTH PHYSICS PROGRAM

OFFICE OF NAVAL RESEARCH

Contract #: N00014-75-C-1126

ACOUSTIC CHARACTERISTICS OF THE SHELVES BETWEEN ALASKA AND U.S.S.R.

by

Robert E. Houtz

L-DGO #: CU-2-79

Technical Report #2

1979

Unclassified

SECURITY CLASSIFICATION OF THIS PAGE *(When Data Entered)*

REPORT DOCUMENTATION PAGE

READ INSTRUCTIONS BEFORE COMPLETING FORM

1. REPORT NUMBER: CU-2-79

2. GOVT ACCESSION NO.:

3. RECIPIENT'S CATALOG NUMBER:

4. TITLE *(and Subtitle)*: Acoustic characteristics of the Shelves between Alaska and U.S.S.R.

5. TYPE OF REPORT & PERIOD COVERED: Technical Report 5/79 to 10/79

6. PERFORMING ORG. REPORT NUMBER:

7. AUTHOR(s): Robert E. Houtz

8. CONTRACT OR GRANT NUMBER(s): N00014-75-C-1126

9. PERFORMING ORGANIZATION NAME AND ADDRESS: L-DGO Palisades, N.Y. 10964

10. PROGRAM ELEMENT, PROJECT, TASK AREA & WORK UNIT NUMBERS:

11. CONTROLLING OFFICE NAME AND ADDRESS: Earth Physics Program, Office of Naval Research, Department of the Navy, Arlington, VA 22217

12. REPORT DATE: 10/79

13. NUMBER OF PAGES: 21

14. MONITORING AGENCY NAME & ADDRESS *(if different from Controlling Office)*:

15. SECURITY CLASS. *(of this report)*: Unclassified

15a. DECLASSIFICATION/DOWNGRADING SCHEDULE: N/A

16. DISTRIBUTION STATEMENT *(of this Report)*:

17. DISTRIBUTION STATEMENT *(of the abstract entered in Block 20, if different from Report)*:

18. SUPPLEMENTARY NOTES:

19. KEY WORDS *(Continue on reverse side if necessary and identify by block number)*: Acoustics, sediments, shelf, sonobuoy, refraction.

20. ABSTRACT *(Continue on reverse side if necessary and identify by block number)*:

Sound velocity characteristics at the seafloor and down to depths of 9-10 km have been generalized from 554 sonobuoy solutions in the Chukchi and Beaufort Seas. Sediment isopachs, contoured seafloor sound velocities, general geology, and velocity-depth functions appear in a set of regional charts.

DD FORM 1 JAN 73 1473 EDITION OF 1 NOV 65 IS OBSOLETE
S/N 0102-LF-014-6601

Unclassified

SECURITY CLASSIFICATION OF THIS PAGE *(When Data Entered)*

T E C H N I C A L R E P O R T

For the

EARTH PHYSICS PROGRAM

OFFICE OF NAVAL RESEARCH

Contract #: N00014-75-C-1126

ACOUSTIC CHARACTERISTICS OF THE SHELVES BETWEEN ALASKA AND U.S.S.R.

by

Robert E. Houtz

Lamont-Doherty Geological Observatory of Columbia University

Palisades, New York 10964

L-DGO #: CU-2-79

Technical Report #2

1979

Introduction

Over one hundred sonobuoys were successfully deployed by the U.S. Geological Survey in the Chukchi and Beaufort seas. Owing to the thick sediments and the good quality of the sonobuoy records, the average sonobuoy yields 5 to 6 layers, ranging up to 10 layers. This work therefore provides a wealth of sound velocity information in an area where little velocity data has been published. The sonobuoys also provide good estimates of minimum sediment thickness (up to 9.6 km), some detail within the basement structure, and sea floor sound velocities.

The chart in Figure 1 shows the location of sonobuoys used in the present work. The sonobuoys obtained during 1977 and 1978 aboard R.V. Lee are indicated with open circles in Figure 1. These data were obtained with military sonobuoys (SSQ41A) and a 5-element tuned array of airguns with a total volume of 1350 in^3. Sonobuoy data were obtained during 1971, 1972, and 1973 by the U.S.C.G.C. Burton Island; these stations are shown as solid circles in the figure. They were shot with a variety of sources including mixed sources where both sparkers and airguns were used.

Generalized sediment provinces and the distribution of eroded arches are shown in Figure 2. This map was adapted from the work of Grantz and Eittreim (1979) and Eittreim et al. (1977). The locations of the structural highs, although approximate, were used to help control contour lines of seafloor sound velocity and sediment thickness wherever control data were scarce.

Reduction of Sonobuoy Data

The sonobuoy records shown in Figure 3 are typical of those used in the present work. For the most part the sonobuoys are located in shallow water, and the travel-time data show a smooth increase of velocity with depth, at least within the upper (sedimentary) refracted arrivals. Deep reflections are commonly observed in the shallow water sonobuoy records. Such a reflector has been labelled "R" in Figure 3. Whenever the computed reflection time to the deepest refracting layer is less than an observed reflector, the thickness of the final layer down to the reflector was computed by assuming a constant velocity equal to that of the deepest refractor. In order to compute the thickness as accurately as possible, in sediments whose velocity increases smoothly with depth, it is necessary to pick as many velocity changes as possible. As a consequence, many of our solutions contain upwards of 10 layers. As a check against these thickness calculations, twelve sonobuoys with well-defined travel-time curvature (without velocity cusps) were inverted by use of the Herglotz-Bateman velocity inversion technique. One such sonobuoy is shown in the left hand side of Figure 3. These results will be discussed in more detail later, but it can be mentioned here that the depths computed from closely spaced refraction picks are in good agreement with the inverted data.

After studying the sonobuoy records it was concluded that the onsets of the low-energy, straight-line refraction arrivals generally occurred at velocities equal to or greater than about 4.5 km/s. At shallower depths the travel-time data are curved, and since they benefit from the focussing effect of a positive velocity gradient, they contain

much more energy. These properties are rather easily identified (see the arrow on the left of Fig. 3) and are the basis for division into 'basement' and sediment in our sections, although the work of Grantz et al., show that over most of the shelf, basement defined in this way is actually sedimentary.

It seems to be a characteristic of shelf sediments whose velocities increase smoothly with depth that dipping reflectors (bedding planes) have little or no effect on the refraction velocity. That is to say, zones of equal sound velocity tend to be horizontal in spite of dipping bedding planes (cf. Houtz and Davey, 1973). This is shown in Figure 4 where sonobuoys 32 and 34 are only a few miles apart: 32 was shot up-dip and 34 was shot down-dip, yet there are no important differences between their velocity structures. Dip corrections have been applied to basement velocities, but only in the very few areas where large velocity contrasts exist between sediment and basement. Typically the contrast is less than 400 m/s and the correction is hardly more than the accuracy of measurement. The independence of refraction velocities from bedding plane dip is a convenient demonstration that simple overburden controls velocity. This implies a lack of significant pelagic content, such as lime or silica, which would yield cemented layers whose refraction velocity would be affected by the dip.

Standard T^2/X^2 techniques were applied to the deep water sonobuoy data in the Canada basin. These solutions, based on variable-angle reflections, yield interval velocities. These solutions are dependent on the dip of the reflectors and must be carefully corrected. All the sonobuoy solutions from the present work are listed in Table 1. Except for a

few deep-water stations, all the sonobuoy solutions are based on conventional refraction techniques.

Sound Velocity Analysis of Sediments

Velocity-depth information was collected from eight regions in the study area where the sediments are thick enough to make meaningful statistical correlations between velocity and depth. The solutions for layer thickness from these areas were converted to time, and each velocity was assigned to the mid-point (in units of one-way travel time) of its layer. Least-squares lines were fitted to the velocity-time data to yield the regression coefficients, standard error of estimate, and correlation coefficient. Results are shown in Figure 5 where each region is outlined and labelled, and the statistical information is listed. Whenever possible, refraction velocities greater than 4.5 km/s were included in the velocity-depth plots, but most of these points fell well above the regression line and cannot be included. Their rejection on the basis of their reduced amplitudes and relative lack of travel-time curvature, as discussed earlier, seems to have been justified.

The velocity data from the western Beaufort sea (areas B, C, D) are similar enough to indicate a common origin, whereas the Canada basin to the north (area E) has a much lower velocity gradient in deep water sediments. The distributions from these study areas have large correlation coefficients, indicating thick and uniform sediments. Areas A and G are identical, but quite distinct from BCD. The principal difference between the two groups is the 40% increase in the acceleration factor (K) in area AG over that of BLD. This difference may only represent

the contrast between proximal (western Beaufort shelf) and distal (North Chukchi basin) sedimentation of materials that are otherwise about the same age and with the same type of provenance.

Earlier results obtained by Hofer and Varga (1972) from Mackenzie Bay 100 km east of area D, show a gradual increase of velocity with depth. Their measurements were based on carefully correlated stacking velocities. The velocity-depth distribution indicated to them that the sediments were likely to be a 'sand-shale sequence of Tertiary and Cretaceous age', whose properties they correlated with on-shore well-log data. They obtained the relation $v = 1.62 + 1.39\ t$ in a single survey line, which compares very favorably with our results: $v = 1.59 + 1.53\ t$ from area D.

During the reduction of the sonobuoy data, it was apparent that many of the records could be more accurately reduced by considering the travel-times as continuously varying rather than as straight line segments. In order to use velocity inversion techniques with a minimum of error, we chose travel-time plots that are devoid of prominent velocity cusps (small cusps, i.e. short 'reversed segments' are not easily identified and have no important effect on the inversions). An example of a prominent velocity cusp appears in the right side of Figure 3, which shows that the high-energy cusp survives the multiple reflection process, whereas the deeper straight-line refraction segment is too weak to persist beyond the first multiple. The water layer multiples of the retrograde and prograde portions of the cusp are labelled A and B, respectively, in the figure. After selecting only those records with

relatively deep ray excursions (maximum depths range from 2.5 to 4 km), and screening those with velocity cusps, 12 high-quality records were inverted by means of the Herglotz-Bateman technique.

These inversions were originally carried out as a check against the conventional refraction solutions, which could yield inaccurate results in a sediment column whose velocity increases smoothly with depth. It was found, however, that there are only random differences between the two techniques if 'layers', as picked from the records, are separated by velocity differences of about 300 m/s. It is worth noting that picking layers that are thin relative to a wavelength in a velocity-depth continuum is entirely valid. Objections are raised if conventional refraction methods are used on thin layers, but no objections are raised if the same procedure is called a tau-p inversion, even though the results and the computing procedures are the same.

The velocity inversions seem to provide additional information if they are plotted in their geographical setting, as portrayed in Figure 5 with insets and lines connecting the plots to the sonobuoy station location. It can be seen that area B velocity-depth plots are all basically linear, whereas those from some of the other areas are more complex, and consist of velocity-depth curves or two quite different linear segments. In each case the near-surface linear segment has a greater velocity gradient than in the deeper one. The change-over point from a high to a low velocity gradient occurs fairly consistently at a velocity of about 3 km/s, but the depth at which this occurs is quite variable.

The interval velocity solutions of Hofer and Varga show a very pro-

nounced change in velocity gradient at 3.0 km/s. This event is associated in their data with a moderately strong reflector within a uniform sedimentary sequence. A spot check of our own records revealed no consistent relation between the vertical reflection records and the change of gradient. Although this change of gradient is important to geo-acoustic modelling, our data do not show it as an identifiable geologic event.

The linearity of the velocity-depth plots from area B indicates that the data would be better fitted with a least-squares line relating velocity and depth (rather than one-way travel-time). However, the standard error of estimate and the correlation coefficient actually degrade when a linear relation is attempted between velocity and depth. These results show that the sonobuoys with linear increases of velocity with depth are not representative of the general velocity structure within area B. (The use of a velocity-time regression, although it produces a curved depth distribution, does not increase the degrees of freedom because both the time and depth regressions are compared in their linear forms.)

Seafloor sound velocities in the study area are contoured in Figure 6. These values were determined by picking the earliest possible headwaves in the sonobuoy records. The first layer picks for the thickness calculations were picked from longer refracting segments and are therefore better representative of the 'layer' velocity, but such velocities are somewhat higher than the estimated seafloor sound velocity. As it turns out the velocity-depth functions projected to the seafloor tend to

yield velocities that are in good agreement with the uppermost headwave values plotted in Figure 6. These statistical projections to the seafloor can sometimes be unrealistic.

A third method has been developed to estimate seafloor sound velocity from multiple seafloor reflections at critical incidence. These reflections and their multiples form the line labelled Vg in the right hand side of Figure 3. The group velocity, Vg, can be converted to seafloor sound velocity with a very simple calculation (Sutton and Maynard, 1971). This method yields an average seafloor velocity of 1.63 km/s (based on 8 observations) in areas B, C, and D; and 1.73 km/s (3 observations) from area G. These values are in convincing agreement with the average values based on uppermost headwaves (cf. Fig. 6).

The distribution of seafloor sound velocities shows an increase in velocity in the region of structural arches. This is quite apparent in the central Chukchi sea where the arch is actually an overthrust (Grantz and Eittreim). The minimum velocities are observed on the outward-building, seaward edges of the shelves, and in the central part of the interior basin. An elongate belt of relatively fast velocities are contoured just west of Mackenzie Bay, which may correspond to the 'broad mid-shelf arches and anticlines expressed in Neogene beds' reported here by Grantz and Eittreim.

Area H (Fig. 4) is quite distinct from the other thick sedimentary accumulations because the seafloor sound velocities here are unusually high. This can be seen in Figure 6, but also in the intercept value of

the Area H velocity function. This seems to be directly related to the fact that area H (foredeep) sediments are no younger than Lower Cretaceous, whereas all the other thick sediments are capped by Neogene sediments that are usually quite thick.

Sediment Distribution

The sediment isopach map in Figure 7 is contoured in units of depth down through velocities of 4.5 km/s. Materials faster than this are sedimentary, but they have rather low velocity gradients, so that they are conveniently separable. The isopach map has been contoured to conform with the generalized structure shown in Figure 2. The sonobuoy solutions have been supplemented with results from Eittreim et al., (1977), Grantz and Eittreim (1979), and Eittreim and Grantz (in press). The additional data were obtained from CDP results and some of their earlier interpretations of the sonobuoys listed in Table 1. These earlier solutions are in good agreement with the results listed in Table 1. They were used to identify reflecting surfaces with refraction velocities greater than 4.5 km/s, which I then extrapolated to add to the number of points to be contoured.

The contours on the southernmost arch are based on the sections of Eittreim et al., which they computed with a velocity function of $v = 1.72 + 2.02\ t$. This function yields rather thicker sections than the area F function shown in Figure 4. However, Eittreim (personal communication) has now revised his estimate downwards, based on the inclusion of CDP solutions, and is in good agreement with the result in the present work.

The contoured depths to layers with refraction velocity greater than 4.5 km/s do not necessarily represent a geological boundary. This is especially true on the western Beaufort shelf near Mackenzie Bay, where the 4.5 km/s refraction velocity is observed at depths of about 3 km sub-bottom, which cuts across Lower Tertiary to Jurassic fold structures.

Constraints on the Near-Seafloor Data

A comparison of the velocity depth plots in Figure 4 shows that the near-seafloor velocity gradients will be largest where the velocity plots are non-linear. Where the plots are linear, the regional velocity functions are fairly reliable. However, there is good evidence in area H and to some extent elsewhere on the northern Chukchi shelf, that the near surface velocity gradients may occasionally be double that predicted by the velocity functions. Ideally the travel-time data from each sonobuoy would be inverted, but the labor of doing so, at present is beyond the scope of this paper.

The present work has demonstrated again that random geophysical measurements, such as seafloor sound velocity become more coherent when considered within the constraints of the regional geology. An example that comes to mind here is the elongate gentle fold on the western Beaufort shelf whose crests show up as a 200 m/s increase in the seafloor sound velocity. Similarly Area H, the Colville foredeep, has seafloor sound velocities that are 300 to 400 m/s faster than those in the other basins; this is directly related to their Cretaceous age compared to the much younger sediments in the other basins.

REFERENCES

Eittreim, S., A. Grantz, and O. Whitney, Cenozoic sedimentation and tectonics of Hope basin, southern Chukchi sea, in The Relationship of Plate Tectonics to Alaskan Geology and Resources, edited by A. Sisson, Alaska Geol. Soc., Anchorage, 1977.

Eittreim, S., and A. Grantz, in Crustal Properties across Passive continental Margins, edited by C. Keen and M. Keen, Special Vol. Tectonophysics (in press).

Grantz, A., and S. Eittreim, Geology and physiography of the continental margin north of Alaska and implications for the origin of the Canada basin, U.S. Geol. Survey Open-File Report 79-288, 1979.

Hofer, H., and W. Varga, Sesimogeologic experience in the Beaufort sea, Geophysics, v. 37, no. 4, p. 605-619, 1972.

Houtz, R., and F. Davey, Seismic profiler and sonobuoy measurements in Ross Sea, Antarctica, J. Geophys. Res., 78, 3448-3468, 1973.

Sutton, G., and L. Maynard, Ocean-Bottom sediment velocity determined from critical range multiple reflections (abstract only), EOS, 52, 4, 1971.

TABLE 1

SOSOBOOT SOLUTIONS FROM THE BEAUFORT AND CHUKCHI SEAS

Station	H1 (km)	H2 (km)	H3 (km)	H4 (km)	H5 (km)	H6 (km)	H7 (km)	H8 (km)	H9 (km)	V2 (km/s)	V3 (km/s)	V4 (km/s)	V5 (km/s)	V6 (km/s)	V7 (km/s)	V8 (km/s)	V9 (km/s)	North Lat.	West Long.
2B71	.02	.20	.34	.21	.41	.22				2.20	2.70	3.00	3.25	3.40	3.65			70-43	161-05
4	.05	.60	.69	2.63						1.85	2.50	5.70	7.20					71-23	167-40
5	.05	.48	.37	.25	.39	.46				2.10	2.70	3.00	3.45	3.85	4.20			70-35	167-15
6	.05	.20								2.95	3.70							69-55	167-35
8	.05	.53	.39	.34						1.85	2.30	2.65	4.65					68-36	168-17
9	.05	.35	.38	.54	.59	.57				1.75	2.05	2.40	2.80	3.10	4.20			67-45	167-51
13	.04	.25	.23							1.85	2.70	3.15						70-56	169-30
14	.05	.34								1.70	2.40							70-56	167-17
1B72	.07	.51								1.80	2.20							72-29	159-00
2	.05	.14	.23	.41						2.00	2.70	3.20	4.20					71-33	159-00
4	.08	.28	.48	.51	.50					1.75	2.00	2.45	2.80	3.00				72-55	161-00
5	.09	.58	.31	.62	.18	.81				1.85	2.20	2.60	2.80	3.00	3.70			73-06	163-10
6	.04	.23	.13	.38	.24	.43				2.00	2.40	2.70	3.05	3.45	3.75			71-05	163-00
7	.04	.15	.25	.38	.37					1.75	2.00	2.20	2.40	2.65				73-08	166-30
8	.05	.08	.52	.45	.38	.37	.45			1.75	2.00	2.35	2.65	3.00	3.35	3.80		72-42	168-00
2B73	.04	.47	.18	.43	.32	.38	.73			1.90	2.05	2.30	2.55	2.80	3.10	3.95		71-04	150-55
3	.03	.32								1.75	1.90							71-05	153-00
5	.15	.41	.28	.34						1.75	1.95	2.30	2.55					71-40	154-05
ZL6	.05	.48	.47							1.85	2.10	4.40						68-54	168-04
3	.03	.28	1.56							2.95	3.60	4.05						69-24	165-49
4	.04	.26	.41	.48	1.33	3.35	1.60			2.20	2.80	3.15	3.80	4.25	5.30	5.80		70-34	162-27
5	.04	.45	.38	1.24	3.51					2.30	3.15	4.75	5.15	5.70				71-36	159-23
6	.06	.29	.41	4.06						2.20	2.85	4.50	6.25					71-41	159-30
7	.21	.25	.49	.64	.83	1.77	2.58			1.80	2.45	2.90	3.60	4.10	4.70	5.60		70-42	165-04
8	.03	.60	.89							(1.9)	5.20	5.80						69-24	168-21
9	.03	1.01	1.02							3.90	4.75	5.30						69-40	169-24
10	.04	1.92	.04							3.60	4.15	6.30						70-20	168-59
11	.02	.25	.80	.87	3.08					2.15	3.00	3.65	5.65	6.55				70-43	168-12
13	.02	.38	.55	.57	.76					1.80	2.25	3.00	3.40	5.60				71-05	167-26
16	.02	.59	.44	.78	.67					1.85	2.50	3.05	3.60	5.10				71-29	166-34
17	.04	.63	.66	.82	.76	.92				1.90	2.40	3.05	3.50	4.10	5.25			71-48	165-47
21	.02	.25	.78	.55	.87	2.05				1.80	2.15	3.05	3.60	4.60	5.60			72-39	164-38
22	.03	.85	.62	1.24	3.30					2.10	2.45	3.50	4.35	5.15				72-24	166-31
23	.03	.56	.65	.59						2.00	2.45	3.05	5.95					71-38	169-25
24	.03									3.75								70-34	171-39
25	.03	1.16	.72	1.72	2.44					2.15	3.10	3.90	4.70	5.60				72-13	171-23
27	.03	.53	.66	.89	1.38	(4.85)				1.85	2.35	3.15	3.85	4.45				72-26	173-31
28	.06	.75	.49	.77	.59	1.02	1.21			1.95	2.55	3.05	3.50	4.00	4.50	4.85		72-55	175-50
29	.02	.20	.44	.45	.85	3.91				2.10	2.70	3.20	3.60	4.20	5.05			70-37	162-03
30	.02	.36	.31	.31	.79	1.42	2.33			2.05	2.60	3.00	3.50	3.90	4.40	5.00		70-46	163-31
31	.02	.75	.57	.85	.97	1.20	1.34	3.23	(2.14)	1.90	2.65	3.30	3.65	4.20	4.80	5.45	6.10	70-56	165-01
32	.02	.74	.41	.57	.87	1.10	.75	1.41		1.85	2.55	3.00	3.60	4.15	4.60	5.00	6.60	71-00	166-02
33	.02	.36	.58	.66	.48	2.10				1.75	2.25	2.90	3.40	5.50	6.45			71-06	167-13
34	.02	.84	.42							2.35	2.85	6.15						71-11	168-33
35	.02	1.74	2.32							4.85	5.40	5.90						70-04	170-45
36	.05									4.80								70-00	170-45
37	.05	.61								4.30	4.75							69-44	170-50
39	.03	.69	.69	.65	1.25	1.52	3.34			1.80	2.25	3.00	3.75	5.35	6.00	7.20		68-13	170-45
ZL9	.03	.58	.53	.43	.47	.57				1.65	2.05	2.40	2.80	3.70	4.45			67-21	166-35
5	3.39	1.23	.48	.43	.50	1.22				2.05	2.36	2.59	2.61	3.58				72-33	144-49
6	3.23	.58	.35	.37	.71	.56	1.50			1.88	2.14	2.25	2.74	2.63	3.25	4.20		72-21	143-27
7	2.72	.92	.70							2.15	2.27							71-50	141-00
9	2.66	.64	1.02	.81	2.40					2.00	2.35	2.89	3.48					71-43	141-00
11	2.46	.74	.85	.74						2.07	2.08	2.39	3.35					71-18	140-58
13	.03	.70	.52	.56	.48	.76	.87	4.23		1.80	2.25	3.00	3.40	5.60				69-50	141-18
14	2.83	.78	.60	1.58	2.61	4.00				1.89	2.27	(3.0)	3.65	4.40	5.30			71-34	142-04
19	.04	.66	.60	.65	1.03					2.00	2.20	2.80	3.30	4.10				70-14	142-50
22	3.27	1.12	1.89							2.18	2.90	3.50						71-45	144-43
25	.03	.82	.30	.36	.59	.91				2.00	2.30	2.80	3.25	3.70	4.30			70-15	144-25
27	.04	.13	.26	.53	.58					1.60	2.20	2.60	3.60	4.30				70-16	143-31
30	.05	.63	.30	.35	.34	1.02	2.38			1.75	2.00	2.25	2.60	2.90	3.35	4.30		70-28	140-59
31	.05	.54	.34	.26	.39	.49	2.64			1.80	2.10	2.40	2.65	2.95	3.35	3.85		70-09	141-33
32	.06	.66	.45	.47	.62	.75	.73	1.11		1.85	2.05	2.25	2.65	3.00	3.35	3.85	4.30	70-22	142-16
33	.03	.81	.50	.51	.77	1.39	2.40			1.90	2.15	2.55	2.90	3.20	4.20	5.00		69-58	142-01
34	.05	.67	.54	.33	.46	.72				1.80	2.00	2.35	2.60	3.00	3.35			70-15	142-01
36	.05	.78	.26	.53	.72	.59	3.89			2.00	2.30	2.70	3.05	3.45	4.35	5.60		70-24	143-17
38	.04	.76	.40	.50	2.15	2.07	5.50			1.85	2.15	2.70	3.55	4.10	4.80	5.30		70-24	145-13
39	.03	.79	.53	1.22	1.21	2.92				1.95	2.50	3.20	4.00	4.35	4.70			70-13	145-29
40	.03	.60	.80	.80	.85					1.70	2.00	2.65	3.10	3.75				70-46	146-25
41	.04	.77	.52	.59	.79	.77	1.54	5.25		1.85	2.10	2.40	2.95	3.50	4.30	4.75	5.50	70-37	146-38
43	.05	.82	.51	.72	.66	.62	1.18			1.80	2.25	2.55	3.10	3.60	4.15	4.65		70-48	146-55
44	.04	1.11	.57	1.07						1.80	2.10	3.10	3.80					70-46	147-33
45	.05	.29	.40	.76	.80					(1.8)	2.05	2.35	2.90	3.40				70-53	147-23
46	3.07	.73	1.00	1.19						1.91	2.64	3.38	3.75					71-35	146-25

	km									km/s									North	West
Station	E1	E2	E3	E4	E5	E6	E7	E8	E9	V2	V3	V4	V5	V6	V7	V8	V9		Lat.	Long.
47	.05	.39	.40	.62	.47	.72				1.80	2.05	2.25	3.05	3.30	3.60				70-57	148-20
48	.04	.60	.62	.65	.21					1.90	2.15	2.80	3.10	3.50					70-57	149-01
49	.05	1.01	.99	(3.75)						1.90	2.70	3.70							71-10	149-17
50	.07	.86	.95	1.16	2.17	3.60				1.95	2.35	3.55	4.30	5.00	6.20				71-12	150-18
51	.05	.35	.36	.41	.52	.50	.75	2.07		1.75	2.00	2.30	2.75	3.00	3.35	3.95	6.15		71-08	150-25
53	.04	.44	.55	.56	.56	(2.70)				1.90	2.20	2.40	2.70	3.35					71-00	149-11
54	.03	.80	.61	.64	.53	.61	1.04	3.74		1.95	2.15	3.10	3.40	3.80	4.40	4.80	5.40		70-56	148-43
57	.04	.53	.83	.64	.72	4.05	2.98			1.80	2.20	2.90	3.45	3.95	4.70	5.15			70-47	147-41
58	.04	.51	.92	.91	1.73	5.47				1.95	2.15	3.00	3.90	4.50	5.15				70-42	147-00
60	.05	.54	1.24	.70	.85	(4.51)				1.85	2.25	3.15	3.85	4.40					70-31	145-32
62	.06	.46	.50	.62	.64	.58				1.75	2.10	2.60	3.10	3.50	4.00				71-17	151-14
63	.03	.46	.44	.70	1.20	2.64				1.70	2.10	2.50	3.30	4.25	5.50				71-09	151-52
64	1.95	1.09	.99	.74						(1.8)	2.35	3.30	3.90						71-56	151-52
65	.06	.29	.35	.73	.29	.38	.52			1.75	2.05	2.30	2.50	2.75	3.15	3.55			71-34	153-03
66	.06	.46	.32	.42	.42	.51	.40			1.70	1.95	2.30	2.65	3.15	3.50	3.75			71-27	153-11
67	.04	.32	.38	.31	.34	.43	.38			1.80	2.10	2.30	2.65	3.05	3.50	3.85			71-16	153-39
68	.04	.33	.36	.37	.47	.54	.67			1.65	1.95	2.20	2.50	3.00	3.50	4.00			71-26	154-08
69	.05	.66	.40	.76	.96	2.70	(3.07)			2.00	2.25	2.60	3.30	3.80	4.30				71-39	154-22
70	.09	.35	.24	.27	.31	.39	.54	.60		1.70	2.00	2.40	2.75	3.10	3.50	3.85	4.60		71-34	155-32
71	.03	.58	.27	.47	.54	.52	1.07	.26		1.75	2.00	2.45	3.00	3.45	3.80	4.25	4.80		71-32	154-59
72	.04	.49	.65	.58	1.06					1.75	2.05	2.75	3.35	3.75					71-38	154-16
73	.08	.60	.37	.33	.35	.76				1.80	2.15	2.40	2.80	3.20	3.55				71-25	153-38
74	.09	.47	.38	.35	.59	.45	.73	1.48	1.14	1.70	1.95	2.20	2.65	3.05	3.50	4.10	4.45/5.10		71-22	153-01
75	.06	.43	.52	.52	.64	.65	1.06	(5.22)		1.70	2.00	2.45	2.90	3.50	4.00	4.35			71-19	152-19
77	.05	.49	.47	.35	2.11	1.05	4.76	2.61		1.85	2.10	2.45	2.85	3.80	4.40	5.45	6.35		71-15	151-36
78	.05	.72	.44	.50	.75	.83	1.45			1.90	2.30	2.70	3.10	3.75	4.15	4.45			71-12	150-58
79	.18	.58	.43	1.15						1.80	2.40	2.75	3.85						72-34	158-04
80	.06	.41	.45	.92	2.13	1.26				1.80	2.45	3.20	4.50	6.00	7.30				72-25	158-29
83	.06	.47	.47	2.77	(3.36)					2.20	2.80	4.15	5.35						71-40	158-20
85	.12	.30	.74							2.35	2.75	5.10							71-26	157-30

Fig. 1. Locations of sonobuoys and geographical names in study area.

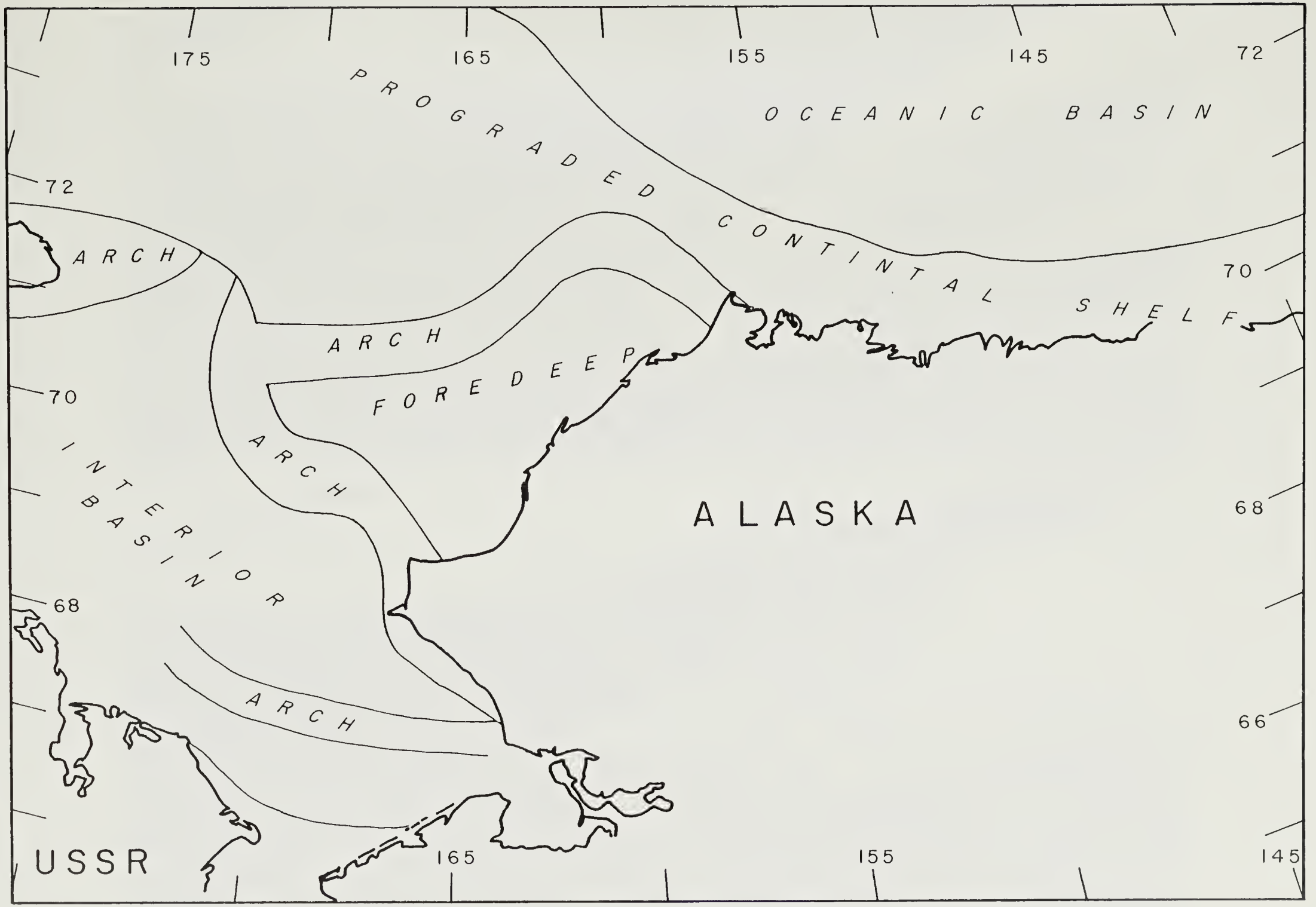

Fig. 2. Geological provinces between Alaska and U.S.S.R.

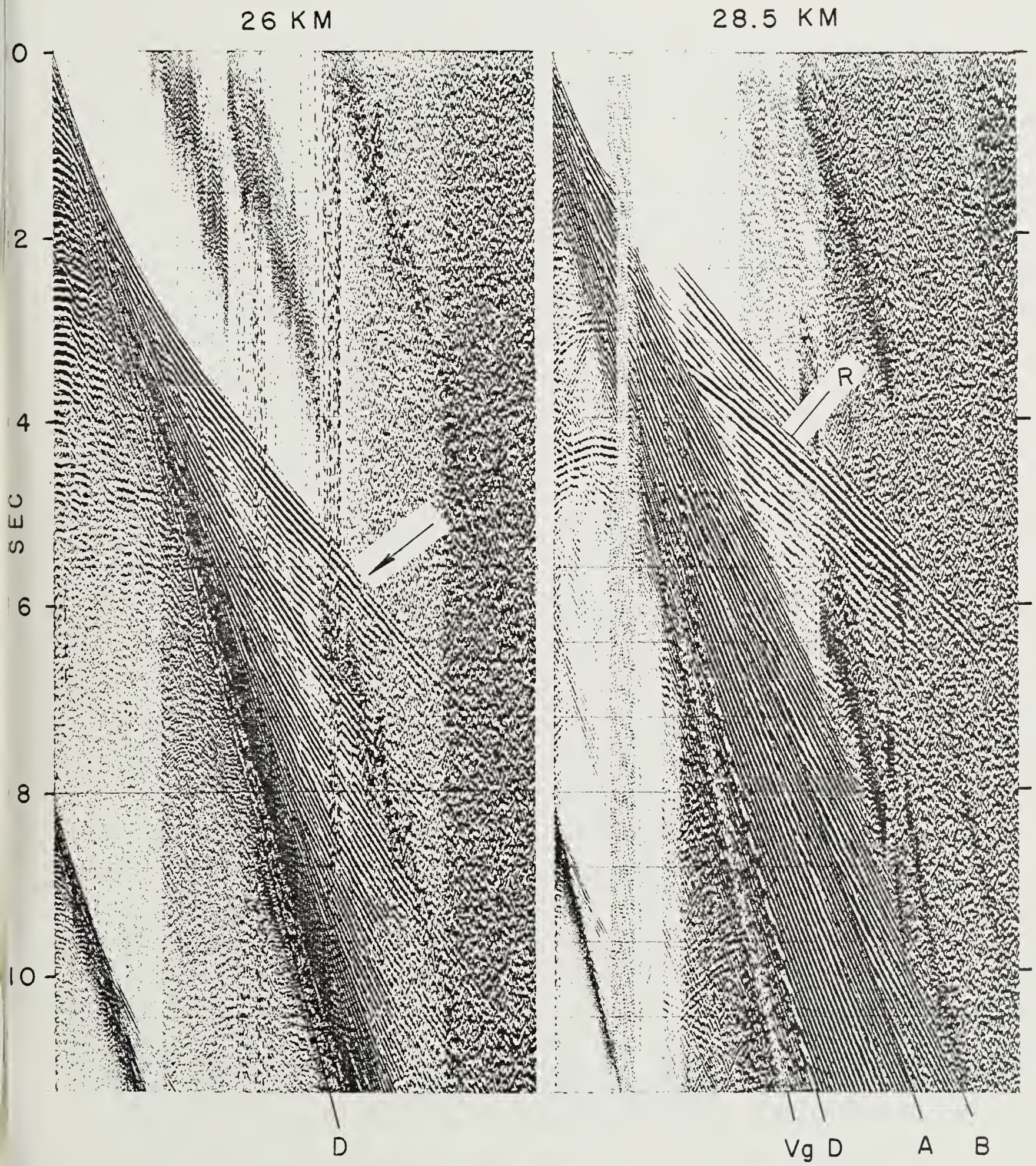

Fig. 3. Sonobuoy records from Chukshi sea. Record on the left shows the transition, marked by an arrow, between curved upper portion of travel-time plot and the weaker straight-line refraction. Deep reflector labelled 'R' on the right. Water layer multiples of critical seafloor reflections (V_g) and prograde and retrograde branches of velocity cusp (B and A, respectively) are identified on the right.

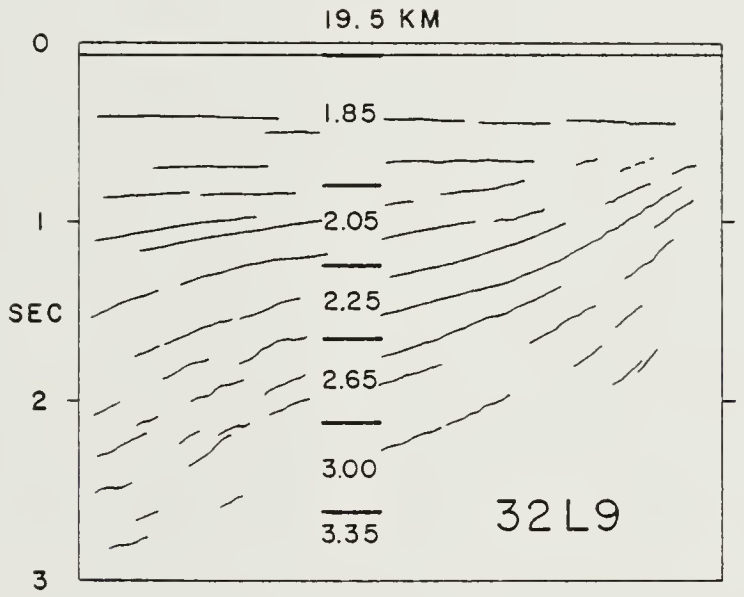

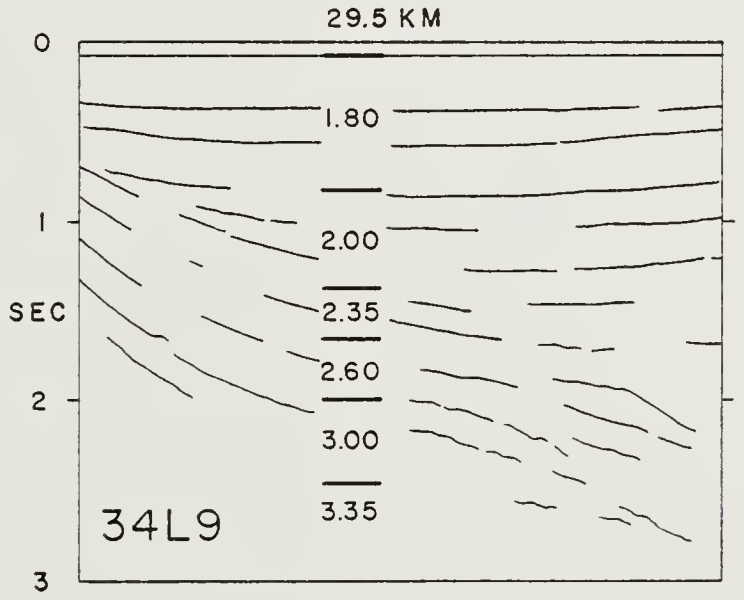

Fig. 4. Refraction solutions obtained from sonobuoy 32L9, shot up-dip, and 34L9, shot down-dip. The nearly identical structure sections demonstrate that the sound velocity depends on overburden and is unaffected by dipping bedding planes.

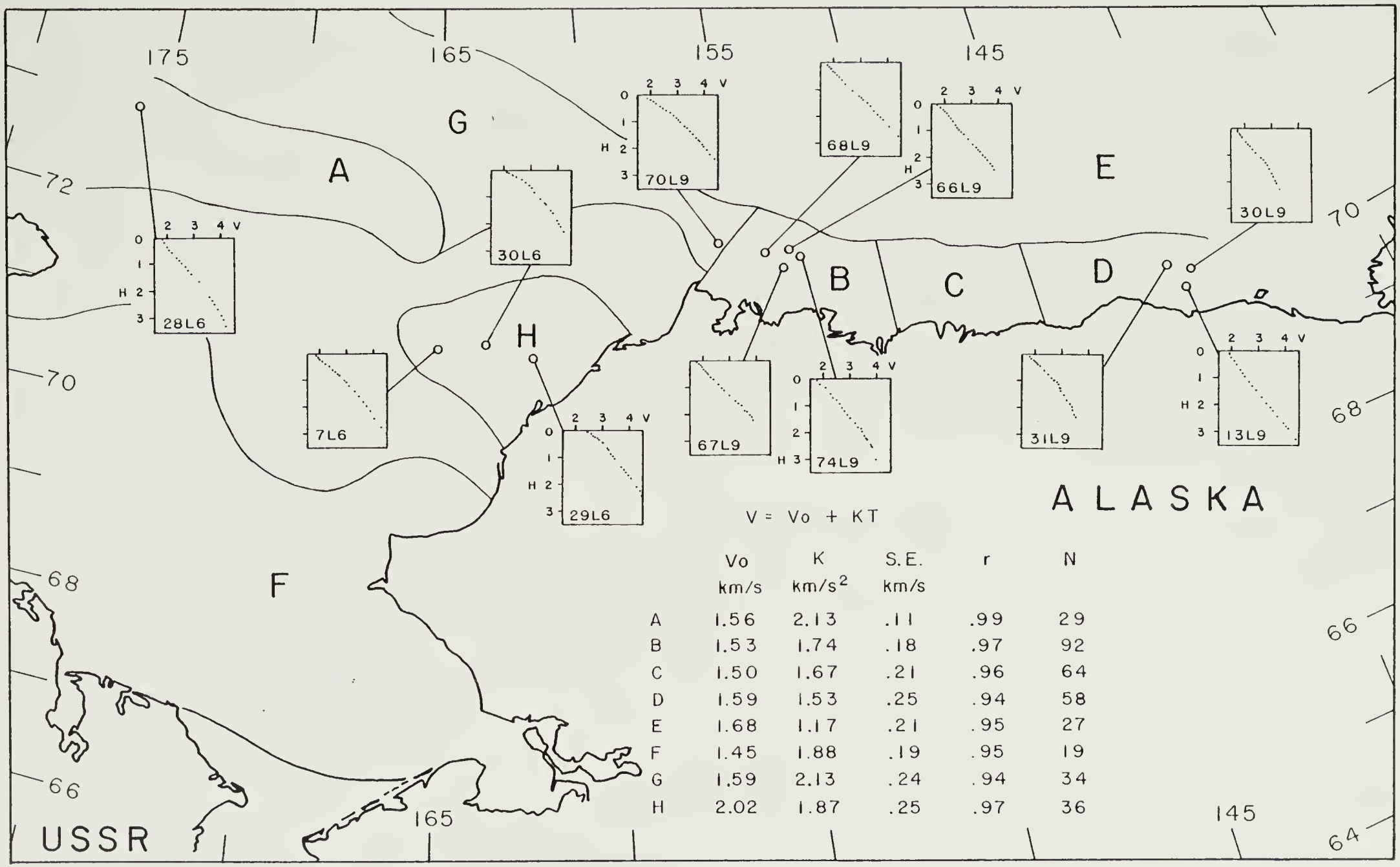

	Vo km/s	K km/s²	S.E. km/s	r	N
A	1.56	2.13	.11	.99	29
B	1.53	1.74	.18	.97	92
C	1.50	1.67	.21	.96	64
D	1.59	1.53	.25	.94	58
E	1.68	1.17	.21	.95	27
F	1.45	1.88	.19	.95	19
G	1.59	2.13	.24	.94	34
H	2.02	1.87	.25	.97	36

Fig. 5. Lettered regions are areas where the velocity functions shown in the table were determined. Insets show selected velocity-depth plots based on travel-time inversions.

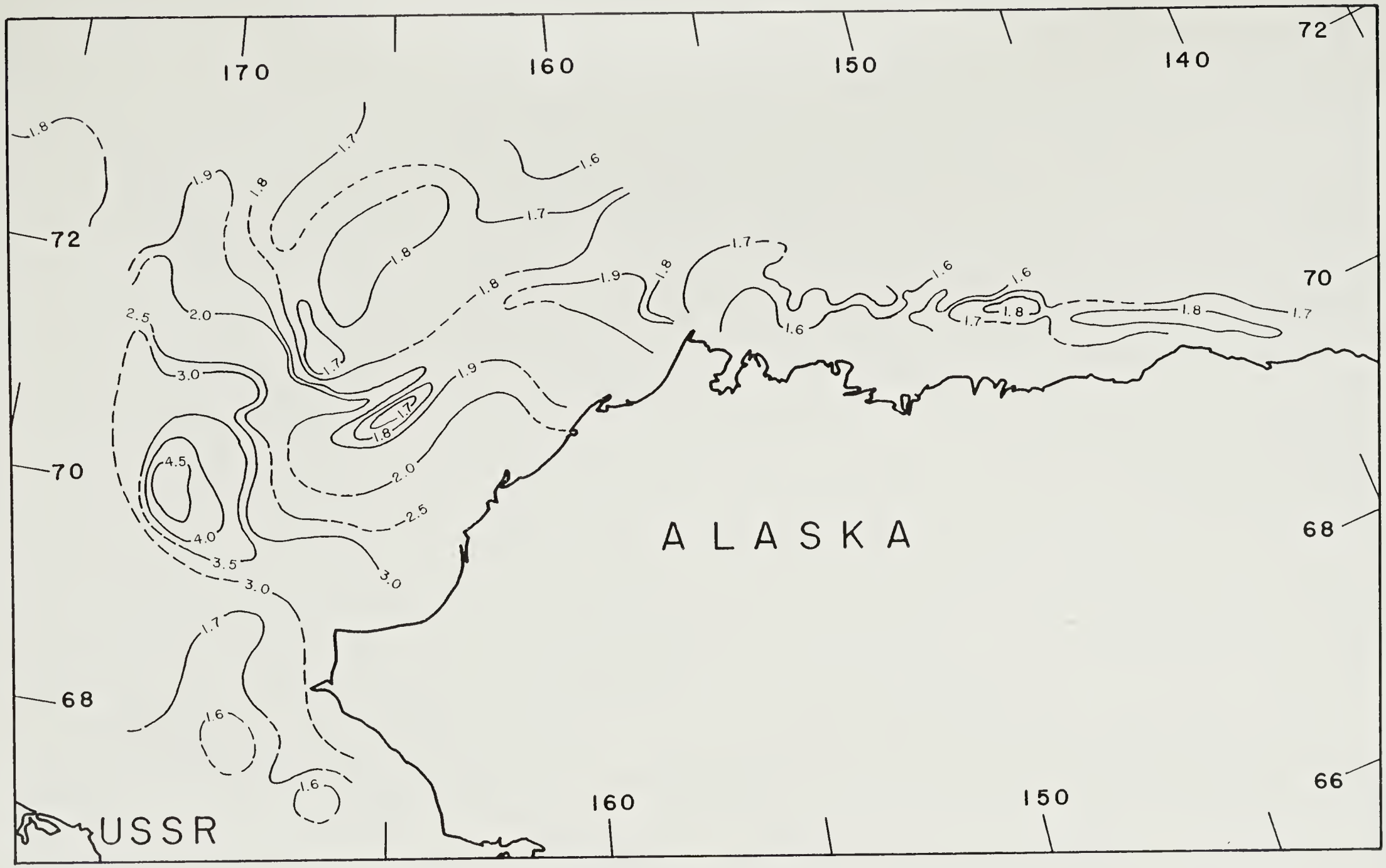

Fig. 6. Seafloor sound velocities contoured in units of km/s.

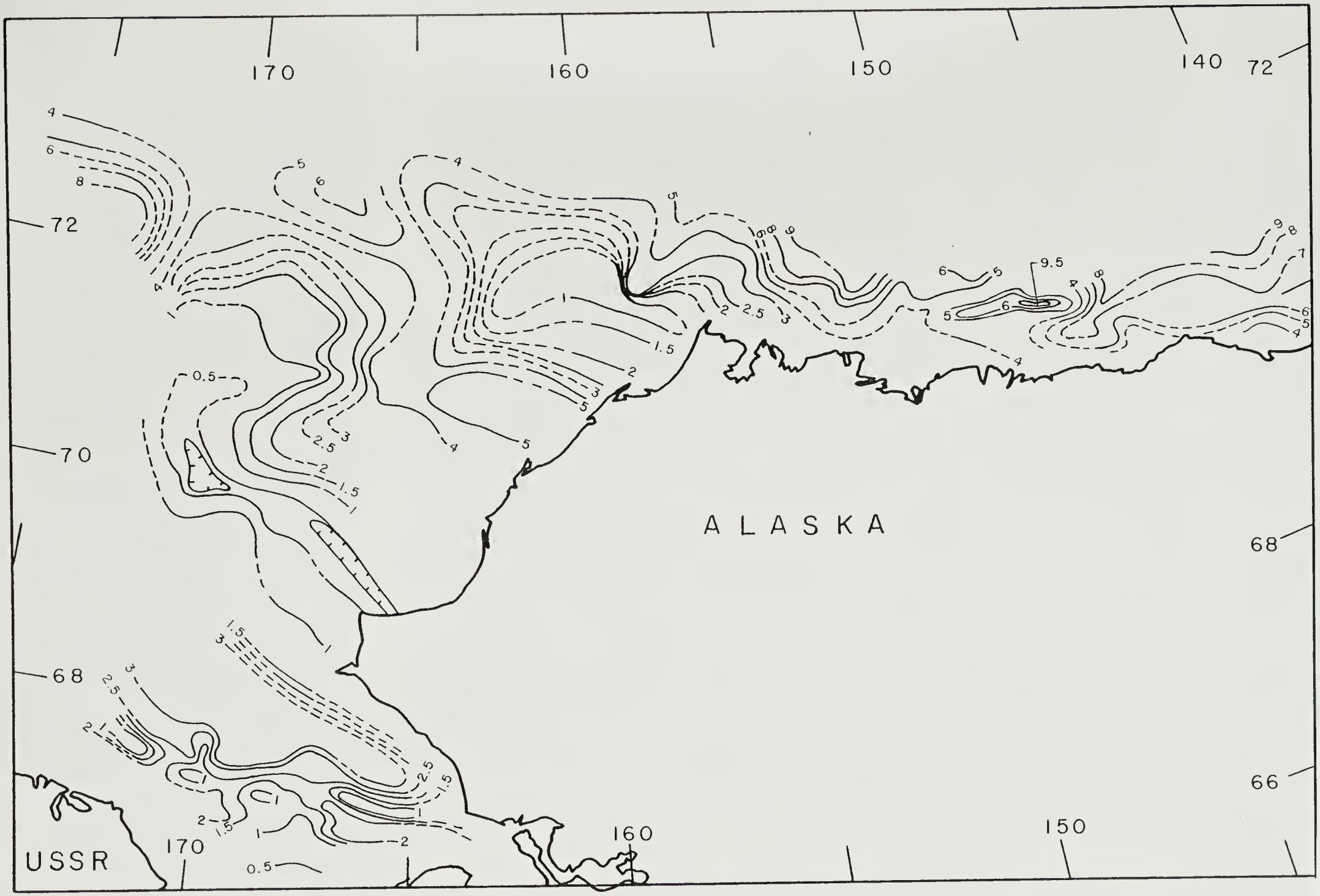

Fig. 7. Sediment thickness contoured in units of km. Hatched areas represent outcrops of high speed materials.